

Modeling global event properties using hydrodynamics from RHIC to LHC

Piotr Bożek

*The H. Niewodniczański Institute of Nuclear Physics, PL-31342 Kraków, Poland
Institute of Physics, Rzeszów University, PL-35959 Rzeszów, Poland*

Abstract. The relativistic hydrodynamic model is applied to describe the expansion of the dense matter formed in relativistic heavy-ion collisions. The hydrodynamic expansion of the fluid, supplemented with the statistical emission of hadrons at freeze-out gives a satisfactory description of the observables for particles emitted with soft momenta. Experimental data for the transverse momentum spectra, elliptic flow and interferometry radii give constraints on the properties of the fluid, its equation of state and viscosity coefficients. The role of the fluctuations of the initial profile of the energy density is discussed.

Keywords: Heavy-ion collisions, hydrodynamic model, collective flow

PACS: 25.75.-q, 25.75.Dw, 25.75.Ld

INTRODUCTION

Experimental studies of heavy-ion collisions at ultrarelativistic energies have the aim at creating a drop of very dense and hot matter and measuring its properties. Measurements at the BNL Relativistic Heavy Ion Collider (RHIC) cover a range of energies up to $\sqrt{s_{NN}} = 200\text{GeV}$ for Cu-Cu and Au-Au systems. Recent results from the CERN Large Hadron Collider (LHC) extend the available energies to $\sqrt{s_{NN}} = 2.76\text{TeV}$ for Pb-Pb interactions.

The results accumulated in the last decade indicate that a fireball of strongly interacting, expanding fluid is formed [1, 2, 3, 4, 5] in the collision. Observables related to the emission of particles with soft momenta demonstrate the onset of a strong collective flow of matter. Particle spectra are written using Fourier coefficients of the directed v_1 , elliptic v_2 , triangular v_3 , or higher harmonic flow

$$\frac{dN}{d^2p_{\perp}dy} = \frac{dN}{2\pi p_{\perp}dp_{\perp}dy} (1 + v_1 \cos(\phi - \Psi_1) + v_2 \cos(2(\phi - \Psi_2)) + v_3 \cos(3(\phi - \Psi_3)) + \dots) . \quad (1)$$

The flow coefficients can be extracted using the orientation angles Ψ or from many-particle cumulants. Transverse momentum spectra of identified particles can be quantitatively understood as coming from the convolution of the collective flow of the fluid elements and of the thermal emission [6, 7]. This observation is even more striking for the azimuthal asymmetry of momentum distributions, the elliptic flow. The observation of the elliptic flow has a very convincing interpretation in terms of the collective expansion of a source with an azimuthally asymmetric initial geometry [8]. Two-particle correlations of same particles allow to measure the interferometry radii of the emission

region [9]. The values of the radii and their dependence on the momentum of the pion pair show the presence of a strong transverse flow. The extracted short emission time points towards a rapid expansion of the fireball.

We discuss the interpretation of the expansion of the fireball in terms of the perfect fluid [10, 11, 12, 13, 14, 15, 16] and viscous hydrodynamics [17, 18, 19, 20, 21, 22]. Many efforts have been devoted to the construction of a model giving a realistic description of the data. These studies yield a dynamical picture of the space-time evolution of the bulk of the matter created in the collision. At the same time they give access to some physical properties of the system, the size and life-time of the fireball, the equation of state, the shear viscosity coefficient. Many unknowns that come into play in the construction of the model, require the use of as many experimental constraints as possible to limit the possible systematic errors. In that way, a satisfactory description of the soft observables limits the effect of the model uncertainties or even helps to get some additional information, e.g on the role of the fluctuations in the initial state.

RELATIVISTIC HYDRODYNAMICS

The expansion of the fireball is described using relativistic hydrodynamics. The basic object in the formalism of second-order viscous hydrodynamics is the energy-momentum tensor [23]

$$T^{\mu\nu} = (\varepsilon + p)u^\mu u^\nu - pg^{\mu\nu} + \pi^{\mu\nu} + \Pi\Delta^{\mu\nu}, \quad (2)$$

the energy-momentum tensor of the perfect fluid gets a correction in the form of the stress tensor $\pi^{\mu\nu}$ from shear viscosity and from bulk viscosity Π , u^μ is the fluid velocity, $\Delta^{\mu\nu} = g^{\mu\nu} - u^\mu u^\nu$. We note, that additional transport coefficients are possible in general [23, 24]. The hydrodynamic equations

$$\partial_\mu T^{\mu\nu} = 0 \quad (3)$$

and the equation of state connecting the pressure p and the energy density ε are supplemented with dynamical equations for the stress corrections

$$\Delta^{\mu\alpha}\Delta^{\nu\beta}u^\gamma\partial_\gamma\pi_{\alpha\beta} = \frac{2\eta\sigma^{\mu\nu} - \pi^{\mu\nu}}{\tau_\pi} - \frac{1}{2}\pi^{\mu\nu}\frac{\eta T}{\tau_\pi}\partial_\alpha\left(\frac{\tau_\pi u^\alpha}{\eta T}\right) \quad (4)$$

and

$$u^\gamma\partial_\gamma\Pi = \frac{-\zeta\partial_\gamma u^\gamma - \Pi}{\tau_\Pi} - \frac{1}{2}\Pi\frac{\zeta T}{\tau_\Pi}\partial_\alpha\left(\frac{\tau_\Pi u^\alpha}{\zeta T}\right). \quad (5)$$

Two viscosity coefficients appear in the equations, the shear viscosity η and the bulk viscosity ζ and two relaxation times τ_π and τ_Π . The value of the viscosity coefficients can be estimated in kinetic theory if the cross sections are known. However, for very strongly interacting systems kinetic theory breaks down [25]. In AdS/CFT calculations the ratio of the shear viscosity to entropy reaches a very small value $\eta/s = 1/4\pi$ [26]. The small value of the shear viscosity, as inferred from the experimental data [1, 2, 3, 4, 5], justifies the use of the perfect fluid hydrodynamics as a first approximation.

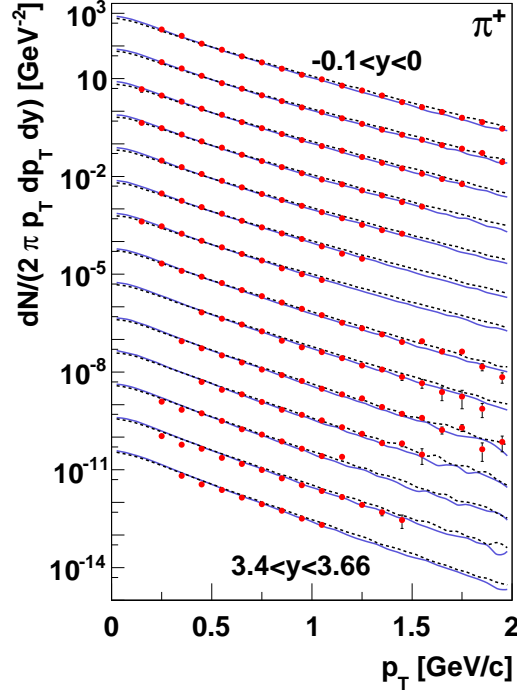


FIGURE 1. Transverse momentum spectra of pions produced in Au-Au collisions at $\sqrt{s} = 200\text{GeV}$ at different rapidities, compared to BRAHMS Collaboration Data [33] (from [16])

Perfect fluid calculations can explain a large number of observations [10, 11, 12, 13, 14, 15, 16, 27]. Calculations have been performed both in simplified, boost-invariant 2 + 1-D geometry as well as in 3 + 1-D. The generation of the transverse flow is correctly described as the acceleration of the collective flow from pressure gradients in the source. The predicted elliptic flow overshoots the experimental points, the calculation can be made closer to the data if a hadronic cascade stage is introduced after the hydrodynamic expansion [27]. The Hanbury Brown-Twiss (HBT) correlations could not be described in early calculations using an equation of state with a first order phase transition [12, 28, 29, 30]. The agreement is greatly improved when using lattice QCD inspired parameterization of the equation of state with a cross over [14, 31].

To illustrate the quality of the predictions of perfect fluid hydrodynamics, we show an example of a 3 + 1-D hydrodynamic simulation [16] with a cross-over equation of state [32]. In Fig. 1 are shown results for the pion spectra at different rapidities. Spectra of pions and kaons can be well described for soft momenta $p_{\perp} < 1.5\text{GeV}$ in a perfect fluid 3 + 1-D model. Up to now, there exist only one calculation of viscous hydrodynamics in 3 + 1-D [22], other viscous codes use the boost-invariant geometry.

We illustrate the sensitivity of the HBT radii, and especially of the ratio R_{out}/R_{side} to the softening of the equation of state. The increase of this ratio has been proposed as a measure of the strength of the first order transition [34]. Experiments at RHIC and the LHC exclude such a behavior. When using the equation of state with minimal softening around T_c (Fig. 2), one obtains the best agreement with the measured interferometry radii

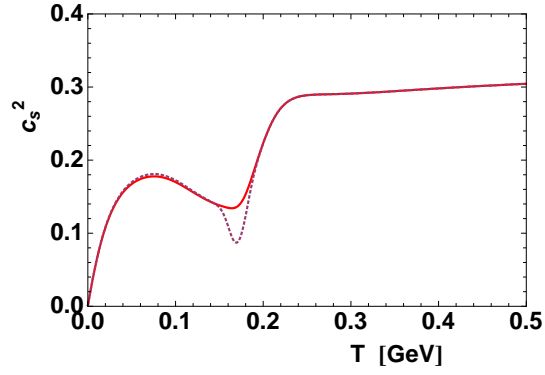


FIGURE 2. Temperature dependence of the square of the velocity of sound, for a cross-over equation of state (solid line) [32] and for an equation of state with a softening around T_c (dashed line) (from [16])

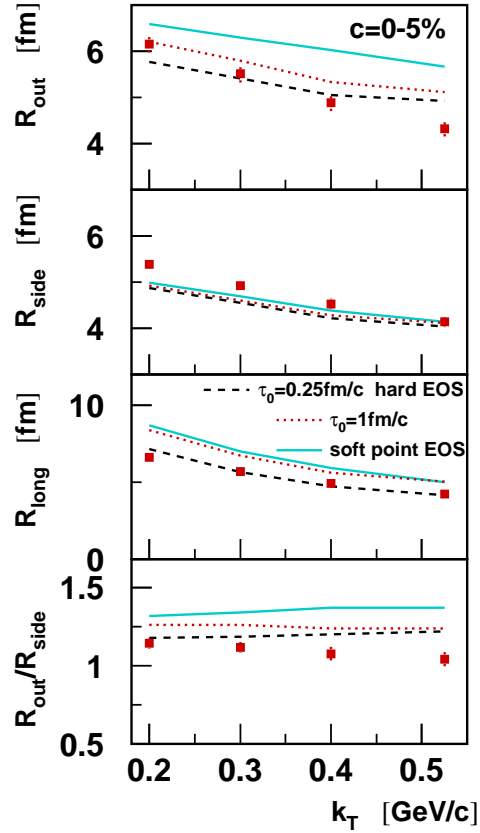


FIGURE 3. HBT radii for hydrodynamic calculation with a cross-over transition (dashed lines) and for an equation of state with some softening around T_c (solid lines) (from [16]).

(Fig. 3). The success of the simulations using a cross-over equation of state [14, 31] is a phenomenological confirmation of recent lattice QCD calculations of the equation of state [35].

The directed flow has been measured at ultrarelativistic energies. The formation of the

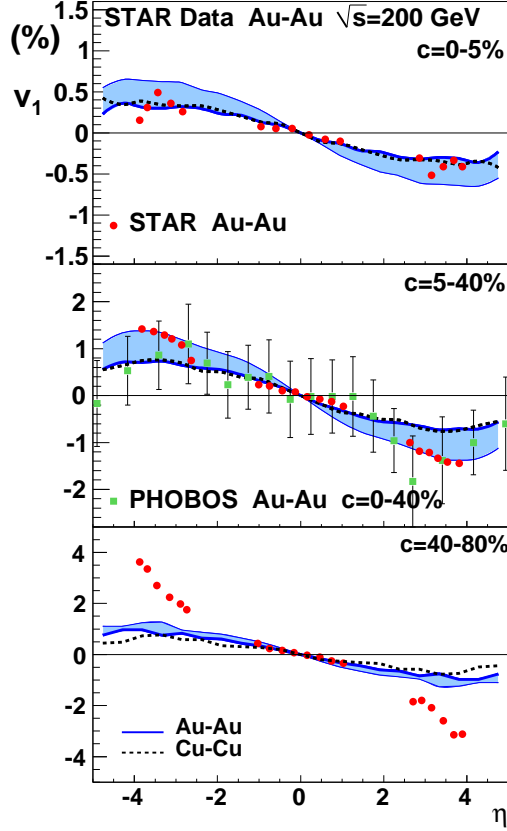


FIGURE 4. Directed flow of charged particles from 3+1-D hydrodynamic calculation, compared to the data of STAR and PHOBOS Collaborations [36, 37]. (from [38]). The color band indicate the systematic error form the range of the uncertainty in the initial tilt of the source.

flow in the hydrodynamic expansion implies a non-boost invariant geometry and requires a mechanism breaking the symmetry around the beam axis. Asymmetric emission from forward and backward going participants [39] leads to a tilt of the source. The model reproduces the observed value of the directed flow, in Au-Au and Cu-Cu collisions (Fig. 4). The formation of the directed flow can serve as probe of the early non-equilibrium imbalance between the longitudinal and transverse pressures [40].

The elliptic flow is generated in the expansion of an initial azimuthally deformed source. The final elliptic flow depends on the time of the evolution, on the viscosity coefficient [41] and on the initial eccentricity. The measured elliptic flow can be used to extract the value of the shear viscosity coefficient [42, 43]. The main uncertainty is related to the value of the initial eccentricity of the fireball. Depending on the assumed model of the initial density profile (Glauber model or KLN model) the extracted value of the shear viscosity lies between $\eta/s = 0.08$ and $\eta/s = 0.2$. The calculation of the elliptic flow for identified particles requires a realistic description of the hadronic stage of the collision [44, 45]. If this stage is modelled by hydrodynamics, bulk viscosity must be introduced. In Fig. 5 the results for v_2 of different particles are shown using $\eta/s = 0.1$

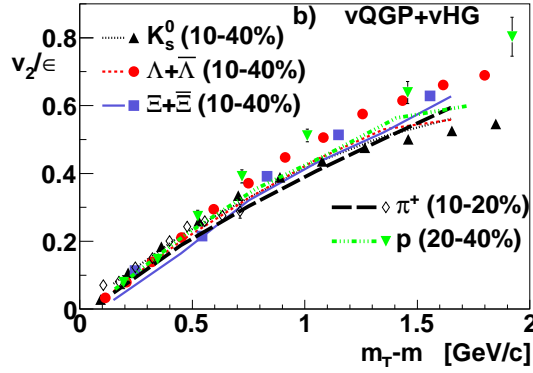


FIGURE 5. Elliptic flow of identified particles scaled by the initial eccentricity in hydrodynamic calculations compared to the data of PHENIX and STAR Collaborations [46], [47], [48] (from [44]).

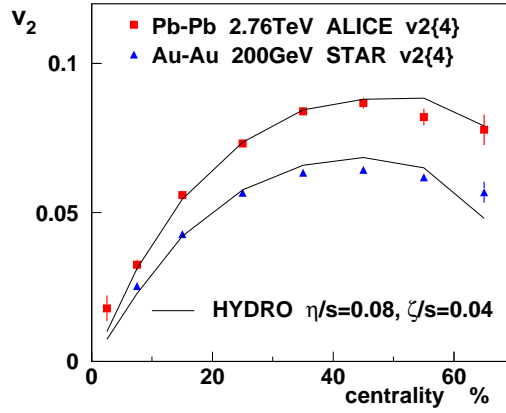


FIGURE 6. Elliptic flow coefficient in Au-Au collisions at $\sqrt{s} = 200\text{GeV}$ (STAR data [48]), and for Pb-Pb collisions at 2.76TeV (ALICE data [5]), compared to viscous hydrodynamics results [49].

and $\zeta/s = 0.04$ in the hadronic phase. In summary, hydrodynamic studies of RHIC data have shown that a strongly interacting matter is formed in the collision, with a cross-over equation of state and a small viscosity. The expansion of the the fireball is very rapid.

FROM RHIC TO LHC

From the recent data on Pb-Pb collisions at the LHC [50, 5] a similar picture of the dynamics emerges as at RHIC energies. The multiplicity and the life-time of the system increases, but the global properties are very similar. In a first approach, the same parameters as used at $\sqrt{s} = 200\text{GeV}$ may be used ($\eta/s = 0.08$ for Glauber initial conditions and $\zeta/s = 0.04$ below T_c) increasing only the initial energy density. Several calculation exist for LHC energies [51, 52, 53, 45, 49, 44, 54, 55]. The elliptic flow of charged particles can be well reproduced (Fig. 6). The spectra of identified particles compared to calculations are shown in Fig. 7. The agreement is satisfactory. However, for light parti-

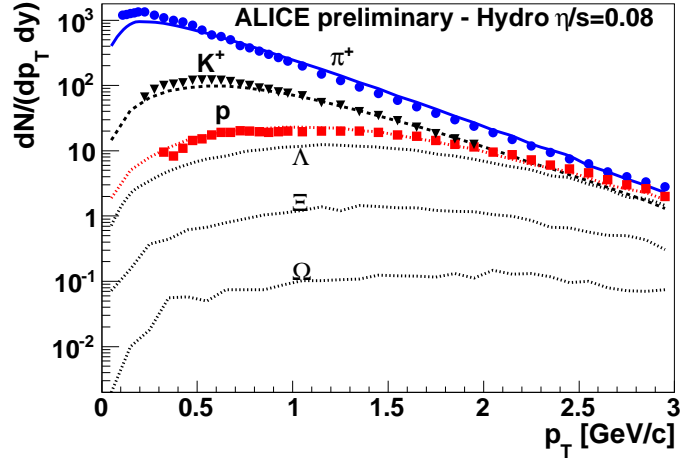


FIGURE 7. Transverse momentum spectra of identified particles from viscous hydrodynamics, compared to preliminary ALICE Collaboration data [56].

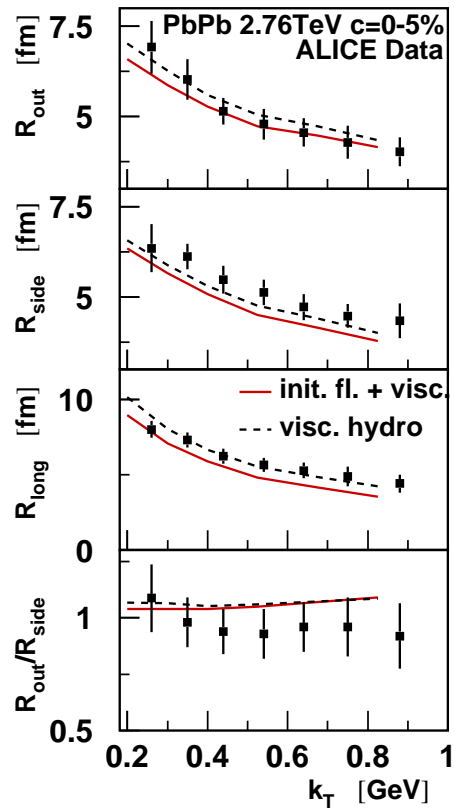


FIGURE 8. HBT radii for pions emitted in Pb-Pb Collisions at $\sqrt{s} = 2.76\text{GeV}$. The hydrodynamic model results are denoted by the dashed lines for zero initial flow and by the solid lines when the initial pre-equilibrium flow is included [44], ALICE Collaboration data [50] (from [44])

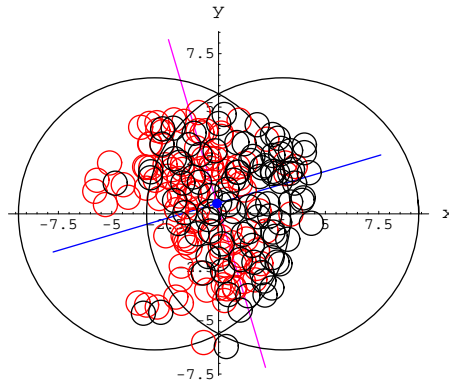


FIGURE 9. Distribution of wounded nucleons in a Glauber Monte-Carlo event, the orientation of the participant plane is rotated with respect to the reaction plane. (from [61])

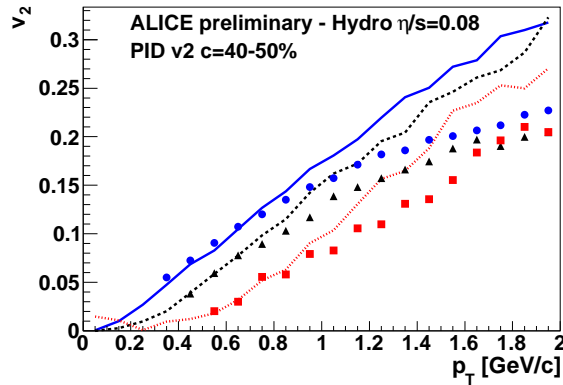


FIGURE 10. Elliptic flow of π^+ , K^+ and p in Pb-Pb collisions, from hydrodynamic calculations compared to ALICE Collaboration data [62].

cles the mean transverse momenta seem too large. The HBT radii can be accounted for by the viscous hydrodynamic calculation (Fig. 8) with the transverse flow generated in the expansion of the fluid. It shows, that the size and the life-time of the system is well understood in dynamical models.

The shape of the initial distribution in the transverse plane (Fig. 9) is largely influenced by fluctuations [57, 58, 59]. As a measure of viscosity effects the triangular flow is especially important [60]. In particular, it is difficult for the model to fit at the same time the elliptic and the triangular flow. Another problem, is to reproduce the mass splitting in the p_{\perp} dependence of v_2 between pions and protons. The elliptic flow of identified particles is reasonably well described (Fig. 10), except for more central events [62]. In Fig. 11 we illustrate the difficulties of the model to reproduce both the strength and the mass splitting of the triangular flow. Some hints of the problems with common predictions for the spectra of pions, kaons and protons is already visible in Fig. 7. It indicates that the very strong transverse collective flow seen at LHC is not entirely accounted for in present hydrodynamic calculations. As noted before, the spectra and the ellip-

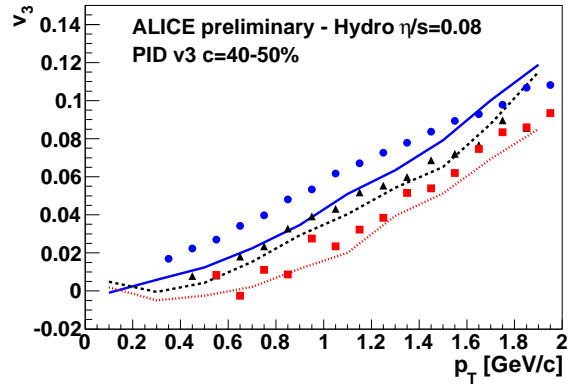


FIGURE 11. Same as Fig. 10 but for triangular flow.

tic flow of identified particles are sensitive also to the final hadronic rescattering. More advanced approaches to fluctuating initial conditions use event by event hydrodynamic calculations [57, 22].

In summary, the hydrodynamic expansion is a realistic description of the behavior of the bulk matter created in relativistic heavy-ion collisions. Viscous hydrodynamics reproduces the observed transverse momentum spectra, the elliptic flow of charged particles and the HBT radii. One can conclude that the hot matter created in the collision behaves like an almost perfect fluid with a cross-over like equation of state. Fluctuations of the shape of the initial state are evidenced in the azimuthal asymmetry of the emitted particles. Some discrepancies remain in the description of the momentum dependence of the elliptic and triangular flows of identified particles.

ACKNOWLEDGMENTS

The work is supported by the Polish Ministry of Science and Higher Education grant No. N N202 263438

REFERENCES

1. K. Adcox, et al., *Nucl. Phys.* **A757**, 184 (2005).
2. I. Arsene, et al., *Nucl. Phys.* **A757**, 1 (2005).
3. J. Adams, et al., *Nucl. Phys.* **A757**, 102 (2005).
4. B. B. Back, et al., *Nucl. Phys.* **A757**, 28 (2005).
5. K. Aamodt, et al., *Phys.Rev.Lett.* **105**, 252302 (2010).
6. E. Schnedermann, J. Sollfrank, and U. W. Heinz, *Phys. Rev.* **C48**, 2462 (1993).
7. F. Retiere, and M. A. Lisa, *Phys.Rev.* **C70**, 044907 (2004).
8. J. Y. Ollitrault, *Phys. Rev.* **D46**, 229 (1992).
9. U. A. Wiedemann, and U. W. Heinz, *Phys. Rept.* **319**, 145 (1999).
10. D. Teaney, J. Lauret, and E. V. Shuryak, *Phys. Rev. Lett.* **86**, 4783 (2001).
11. P. F. Kolb, and U. W. Heinz, "Hydrodynamic description of ultrarelativistic heavy-ion collisions," in *Quark Gluon Plasma 3*, edited by R. Hwa, and X. N. Wang, World Scientific, Singapore, 2004, nucl-th/0305084.

12. T. Hirano, and K. Tsuda, *Phys. Rev.* **C66**, 054905 (2002).
13. Y. Hama, et al., *Nucl. Phys.* **A774**, 169 (2006).
14. W. Broniowski, M. Chojnacki, W. Florkowski, and A. Kisiel, *Phys. Rev. Lett.* **101**, 022301 (2008).
15. P. Huovinen, and P. V. Ruuskanen, *Ann. Rev. Nucl. Part. Sci.* **56**, 163 (2006).
16. P. Bożek, and I. Wyskiel, *Phys. Rev.* **C79**, 044916 (2009).
17. D. A. Teaney (2009), arXiv:0905.2433.
18. P. Romatschke, *Int. J. Mod. Phys.* **E19**, 1 (2010).
19. H. Song, and U. W. Heinz, *J. Phys.* **G36**, 064033 (2009).
20. P. Bożek, *Phys. Rev.* **C81**, 034909 (2010).
21. J.-Y. Ollitrault (2010), arXiv:1008.3323.
22. B. Schenke, S. Jeon, and C. Gale, *Phys. Rev. Lett.* **106**, 042301 (2011).
23. W. Israel, and J. Stewart, *Annals Phys.* **118**, 341 (1979).
24. R. Baier, P. Romatschke, D. T. Son, A. O. Starinets, and M. A. Stephanov, *JHEP* **04**, 100 (2008).
25. P. Danielewicz, and M. Gyulassy, *Phys. Rev.* **D31**, 53 (1985).
26. P. K. Kovtun, D. T. Son, and A. O. Starinets, *Phys. Rev. Lett.* **94**, 111601 (2005).
27. T. Hirano, U. W. Heinz, D. Kharzeev, R. Lacey, and Y. Nara, *Phys. Lett.* **B636**, 299 (2006).
28. C. E. Aguiar, Y. Hama, T. Kodama, and T. Osada, *Nucl. Phys.* **A698**, 639 (2002).
29. K. Morita, and S. Muroya, *Prog. Theor. Phys.* **111**, 93 (2004).
30. K. Morita, *Braz. J. Phys.* **37**, 1039 (2007).
31. S. Pratt, *Phys. Rev. Lett.* **102**, 232301 (2009).
32. M. Chojnacki, and W. Florkowski, *Acta Phys. Polon.* **B38**, 3249 (2007).
33. I. Arsene, et al., *Phys. Rev. Lett.* **91**, 072305 (2003).
34. D. H. Rischke, and M. Gyulassy, *Nucl. Phys.* **A608**, 479 (1996).
35. Y. Aoki, G. Endrodi, Z. Fodor, S. D. Katz, and K. K. Szabo, *Nature* **443**, 675 (2006).
36. B. B. Back, et al., *Phys. Rev. Lett.* **97**, 012301 (2006).
37. B. I. Abelev, et al., *Phys. Rev. Lett.* **101**, 252301 (2008).
38. P. Bożek, and I. Wyskiel, *Phys. Rev.* **C81**, 054902 (2010).
39. A. Białas, and W. Czyż, *Acta Phys. Polon.* **B36**, 905 (2005).
40. P. Bozek, and I. Wyskiel-Piekarska, *Phys. Rev.* **C83**, 024910 (2011).
41. D. Teaney, *Phys. Rev.* **C68**, 034913 (2003).
42. M. Luzum, and P. Romatschke, *Phys. Rev.* **C78**, 034915 (2008).
43. H. Song, S. A. Bass, U. W. Heinz, T. Hirano, and C. Shen (2010), *Phys. Rev. Lett.* **106**, 192301 (2011).
44. P. Bozek, *Phys. Rev.* **C83**, 044910 (2011).
45. H. Song, S. A. Bass, and U. Heinz, *Phys. Rev.* **C83**, 054912 (2011).
46. J. Adams, et al., *Phys. Rev. Lett.* **95**, 122301 (2005).
47. S. S. Adler, et al., *Phys. Rev. Lett.* **91**, 182301 (2003).
48. J. Adams, et al., *Phys. Rev.* **C72**, 014904 (2005).
49. P. Bozek, *Phys. Lett.* **B699**, 283 (2011).
50. K. Aamodt, et al., *Phys. Lett.* **B696**, 328 (2011).
51. M. Luzum, *Phys. Rev.* **C83**, 044911 (2011).
52. B. Schenke, S. Jeon, and C. Gale, *Phys. Lett.* **B702**, 59 (2011).
53. C. Shen, U. W. Heinz, P. Huovinen, and H. Song (2011), arXiv:1105.3226.
54. Y. Karpenko, and Y. Sinyukov (2011), arXiv:1107.3745.
55. H. Niemi, G. S. Denicol, P. Huovinen, E. Molnar, and D. H. Rischke, *Phys. Rev. Lett.* **106**, 212302 (2011).
56. M. Floris, et al. (ALICE) (2011), arXiv:1108.3257.
57. R. P. G. Andrade, F. Grassi, Y. Hama, T. Kodama, and W. L. Qian, *Phys. Rev. Lett.* **101**, 112301 (2008).
58. B. Alver, et al., *Phys. Rev.* **C77**, 014906 (2008).
59. B. Alver, and G. Roland, *Phys. Rev.* **C81**, 054905 (2010).
60. B. H. Alver, C. Gombeaud, M. Luzum, and J.-Y. Ollitrault, *Phys. Rev.* **C82**, 034913 (2010).
61. W. Broniowski, P. Bożek, and M. Rybczyński, *Phys. Rev.* **C76**, 054905 (2007).
62. M. Krzewicki, et al. (ALICE) (2011), arXiv:1107.0080.